Available online at www.sciencedirect.com
SCIENCE DIRECT
Polymer 47 (2006) 4261–4268
polymer
www.elsevier.com/locate/polymer

An alternating low band-gap polyfluorene for optoelectronic devices

Erik Perzon [a,*], Xiangjun Wang [b], Shielis Admassie [b], Olle Inganäs [b], Mats R. Andersson [a]

[a] Polymer Technology, Department of Chemical and Biological Engineering, Chalmers University of Technology, SE-412 96 Gothenburg, Sweden
[b] Biomolecular and Organic Electronics, (IFM), Linköping University, SE-581 83 Linköping, Sweden

Received 20 December 2005; received in revised form 24 March 2006; accepted 30 March 2006
Available online 2 May 2006

Abstract

An alternating polyfluorene (APFO) with low band-gap segments named APFO-Green1 has been designed and synthesized for use in optoelectronic devices. The low band-gap segment consists of an electron acceptor (A), fenced by electron donors (D). This D–A–D configuration leads to a partial charge transfer in the polymer backbone, and thereby a low band-gap (1.3 eV). Results obtained from characterization of APFO-Green1 include light absorption and emission at extended wavelengths as well as high hole mobility. Furthermore, blends of the polymer with different fullerene derivatives exhibit unusually high photovoltaic performance at long wavelengths, making this type of conjugated polymers promising for plastic solar cell applications.

Keywords: Conjugated polymers; Polymer synthesis; Plastic solar cells

1. Introduction

In 1990, Burroughes et al. showed that by applying a voltage through a thin film of an undoped conjugated polymer, light-emission (electro-luminescence) could be induced [1]. This discovery made it possible to produce polymer light-emitting diodes (PLEDs) and today, the focus has shifted from doped, electrically conducting conjugated polymers to undoped, semiconducting ones. Light-emitting diodes and color displays with conjugated polymers as active materials are starting to gain commercial foothold and several other applications such as lasers [2], transistors [3] and solar cells [4] are being developed rapidly. Today, the main focus in the field is on aromatic polymers such as; poly(*p*-phenylenevinylene) [5], polyfluorene [6], polyaniline [7], and polythiophene [8]. These types of polymers are relatively stable and many of their features can be tuned by the incorporation of different substituents.

At present, it has become more or less a necessity to make sure that newly synthesized conjugated polymers are soluble. The main reason for this requirement lies in the fact that a soluble material can be deposited by fairly uncomplicated means, such as spin-casting [9] or standard printing techniques (e.g. offset- or ink-jet printing) [10,11]. This could make it possible to develop cheap, large-area electronic devices on flexible substrates like paper or plastic foil [12–14].

The field of solar cells based on conjugated polymers is subject to intensive academic, as well as industrial research and recently, overall efficiencies in the region of 5% with reasonable lifetimes under simulated sunlight have been reported [15,16]. In these devices, the active layers are made up of composites of a conjugated polymer, poly(3-hexylthiophene) and a derivative of the Buckminster fullerene called PCBM [17]. Despite the fact that poly(3-hexylthiophene):PCBM solar cells are the most efficient reported so far, they only cover wavelengths up to about 650 nm. To harvest a larger fraction of the solar photon flux and achieve photovoltaic response reaching into the NIR and IR regions, polymers with narrow band-gaps that absorb light at longer wavelengths are needed.

In conjugated polymers, the band-gap determines, which wavelengths of light are absorbed and emitted by the material. Among the factors that influence the band-gap of a polymer are; conjugation length, solid-state ordering, and the presence of electron-withdrawing or -donating moieties. Therefore, by modifying one or more of these properties, polymers with controlled band-gaps and thus, specific optical and electrical characteristics can be synthesized. The effective conjugation length, which is dependent upon the torsion angle between the repeating units along the polymer backbone, can be controlled by choosing sterically hindered units along the polymer

* Corresponding author. Tel.: +46 31 7723402; fax: +46 31 7723418.
E-mail address: perzon@chalmers.se (E. Perzon).

0032-3861/$ - see front matter © 2006 Elsevier Ltd. All rights reserved.
doi:10.1016/j.polymer.2006.03.110

backbone or by introducing bulky side-chains to twist the units out of plane [18]. By different heat- or vapor-treatments, it has been shown that the solid state order and therefore, the band-gap in a polymer film can be modified [19,20]. If electron-donating or -withdrawing side groups are attached to the polymer backbone, the energy levels of the HOMO and/or the LUMO can be altered to control the band-gap [21–23].

Besides attaching electron-donating or -accepting substituents as side groups, band-gap control can be achieved by incorporating alternating donor (D) and acceptor (A) moieties in the polymer main-chain. This causes a partial charge-separation along the polymer backbone, which gives the polymer a lower band-gap [19]. Several monomers and polymers in this category have previously been synthesized and evaluated [19,24–26]. It has recently been shown that polymers of this kind, in blends with PCBM, can exhibit fairly efficient photovoltaic behavior up to about 800 nm [26–28] and extend into even longer wavelengths, but so far only with very low efficiencies [25]. The best solar cell polymers utilizing the donor–acceptor approach published to date are the alternating copolymers of donor–acceptor–donor (D–A–D) segments and dialkylated fluorene segments reported by Svensson et al. [29–31]. The choice of the fluorene unit in these polymers was motivated by the fact that polyfluorenes have shown good stability [32–34] and can form liquid crystalline phases [35], which improve charge mobility.

In this paper, the design, synthetic procedure and properties of a low band-gap polymer, APFO-Green1 (Scheme 2), is reported together with a brief summary of different devices made from the polymer. More detailed descriptions of devices from APFO-Green1 have been published previously [36–40]. APFO-Green1 was designed with the ambition of preparing a polymer that exhibit the advantages of previously published alternating D–A–D polyfluorenes [29–31], while extending the light absorption and photovoltaic response into even longer wavelengths. By introducing a stronger acceptor unit compared to those in Svensson's polymers [29], while still maintaining planarity along the polymer backbone, the D–A–D nature of the low band-gap segment can be further accentuated [24]. In APFO-Green1, the low band-gap D–A–D segment has been emphasized through the introduction of a [1,2,5]thiadiazolo[3,4-*g*]quinoxaline moiety, which is a strong electron acceptor and yields a significant decrease in band-gap [19,24].

2. Experimental section

2.1. Synthetic procedures

2.1.1. 4,7-Dibromo-5,6-dinitro-benzo[1,2,5]thiadiazole (II)

To a mixture of fuming sulphuric acid (100 ml) and fuming nitric acid (100 ml) at 0 °C, 4,7-dibromo-benzo[1,2,5]thiadiazole (**I**) (20 g, 68 mmol) was added in small portions. The reaction mixture was allowed to reach room temperature and after 72 h of stirring, it was poured into ice-water (500 ml). The resulting greenish-yellow slurry was filtered and the residue was washed with water. The filter cake was recrystallized in ethanol to give 7.63 g (29%) of 4,7-dibromo-5,6-dinitro-benzo[1,2,5]thiadiazole (**II**) as pale yellow crystals. Melting point: 198 °C.

2.1.2. 4,7-Di-thiophen-2-yl-5,6-dinitro-benzo[1,2,5]thiadiazole (III)

A solution of 4,7-dibromo-5,6-dinitro-benzo[1,2,5]thiadiazole (**II**) (3.82 g, 9.95 mmol) and 2-(tribytylstannyl)thiophene (9.28 g, 24.8 mmol) in freshly distilled THF (50 ml) was degassed and put under a nitrogen atmosphere. The mixture was heated to reflux and dichlorobis(triphenylphosphine)-palladium(II) (140 mg, 0.2 mmol) dissolved in freshly distilled, degassed THF (5 ml) was added via a syringe. After 4 h, an orange precipitate had formed and the heating was removed. When the mixture had cooled to room temperature, the precipitate was filtered off and washed with petroleum ether. Since, the crude product contained traces of 2-(tribytylstannyl)thiophene, it was dissolved in boiling THF and precipitated by the addition of petroleum ether. The precipitate was filtered and washed with petroleum ether to give pure **III** (3.56 g, 92%) as an orange powder. ^{1}H NMR (300 MHz, $CDCl_3$): δ 7.24 (t, 2H), 7.52 (d, 2H), 7.75 (d, 2H).

2.1.3. 4,7-Di-thiophen-2-yl-benzo[1,2,5]thiadiazole-5,6-diamine (IV)

A slurry of 4,7-di-thiophen-2-yl-5,6-dinitro-benzo[1,2,5]thiadiazole (**III**) (500 mg, 1.28 mmol) and fine iron powder (850 mg) in acetic acid (25 ml) was stirred 3.5 h at 80 °C. The reaction mixture was cooled to room temperature, precipitated in 5% aqueous NaOH (100 ml) and extracted three times with diethyl ether (100 ml). The combined organic layers were washed twice with brine (300 ml), dried with magnesium sulphate and the solvent was removed on a rotary evaporator. This gave 422 mg (100%) of **IV** as golden brown flakes. ^{1}H NMR (300 MHz, $CDCl_3$): δ 4.40 (s, 4H), 7.26 (t, 2H), 7.37 (d, 2H), 7.57 (d, 2H).

2.1.4. 6,7-Diphenyl-4,9-dithien-2-yl-[1,2,5]thiadiazolo[3,4-g]-quinoxaline (V)

To a slurry of 4,7-di-thiophen-2-yl-benzo[1,2,5]thiadiazole-5,6-diamine (**IV**) (2.4 g, 7.3 mmol) in acetic acid (400 ml), benzil (3.1 g, 14.7 mmol) was added in one portion. The mixture was stirred at room temperature over night after which thin-layer chromatography on silica gel with dicloromethane as eluent showed no traces of diamine (**IV**). Acetic acid was removed on a rotary evaporator and the residue was recrystallized in ethanol to remove excess benzil. This gave 3.25 g (89%) of the desired product (**V**) as a dark blue–green powder. ^{1}H NMR (300 MHz, $CDCl_3$): δ 7.33 (t, 2H), 7.38–7.46 (m, 6H), 7.70 (d, 2H), 7.81 (dd, 4H), 9.02 (d, 2H).

2.1.5. 6,7-Diphenyl-4,9-bis-(5-bromo-thiophen-2-yl)-[1,2,5]thiadiazolo[3,4-g]quinoxaline (VI)

A solution of 6,7-diphenyl-4,9-dithien-2-yl-[1,2,5]thiadiazolo[3,4-*g*]quinoxaline (**V**) (2.25 g, 4.46 mmol) in a (1:1) mixture of chloroform and acetic acid was prepared by initially dissolving **V** in 125 ml refluxing chloroform and after allowing the solution to cool to room temperature adding 125 ml acetic

acid. Two equivalents of *N*-bromosuccinimide (1.59 g, 8.92 mmol) were added and the mixture was stirred in darkness at room temperature for 2.5 h. At this point, a dark blue–green precipitate had formed. Thin-layer chromatography on silica gel with dicloromethane as eluent indicated complete reaction and 20 ml methanol was added to facilitate further precipitation. The product was collected by filtration and washed with methanol to yield 2.77 g (94%) of pure **VI** as a dark blue–green powder. ^{1}H NMR (300 MHz, $CDCl_3$): δ 7.25 (d, 2H), 7.41–7.50 (m, 6H), 7.74 (dd, 4H), 8.92 (d, 2H).

2.1.6. Polymerization of APFO-Green1

The monomers; 6,7-diphenyl-4,9-bis-(5-bromo-thiophen-2-yl)-[1,2,5]thiadiazolo-[3,4-*g*]quinoxaline (**VI**) (1.19 g, 1.79 mmol) and 2,7-bis(4′,4′,5′,5′-tetramethyl-1′,3′,2′-dioxaborolan-2′-yl)-9,9-dioctylfluorene (**VII**) [41] (1.15 g, 1.79 mmol) were dissolved in degassed, refluxing toluene (50 ml) and put under a nitrogen atmosphere. A suspension of tetrakis(triphenylphosphine)Pd(0) (400 mg, 35 μmol) in 5 ml degassed toluene was added through a syringe, followed by the addition of degassed tetraethylammonium hydroxide (5.0 ml, 20 wt% in water, 7.0 mmol). After 1 h reflux, another portion of tetrakis(triphenylphosphine)Pd(0) (100 mg, 9 μmol) suspended in 5 ml degassed toluene was added through a syringe. After three more hours, bromobenzene (280 mg, 1.79 mmol) was added through a syringe and was allowed to react for 1 h, whereupon phenylboronic acid (218 mg, 1.79 mmol) was added. One hour after the addition of phenylboronic acid, the reaction mixture was allowed to cool to room temperature and was poured into 200 ml methanol. The precipitated polymer was collected on a PTFE membrane filter with 0.5 μm pore size and dissolved in 100 ml boiling chloroform. After being allowed to cool to room temperature, the polymer solution was stirred over night with ammonia (100 ml, 25% aqueous solution) to remove catalyst remnants and other impurities. The phases were separated and the organic layer was washed over night once more with ammonia (100 ml, 25% aqueous solution). After the two ammonia fractions had been combined, they were extracted with 100 ml boiling chloroform. The combined organic phases were then washed two times with 100 ml water. After pouring the chloroform solution into 200 ml methanol, the precipitated polymer was collected on a PTFE filter as described above and suspended in 200 ml diethyl ether to dissolve low molecular weight oligomers. The ether slurry was poured through an extraction thimble, which was Soxhlet extracted with diethyl ether over night, upon which the extracts were practically colorless. To isolate the chloroform soluble fraction of the polymer, the ether soaked thimble was allowed to dry in ambient conditions after which it was Soxhlet extracted with chloroform. The chloroform solution was concentrated to approximately 20 ml and was poured into 200 ml of methanol. After the mixture had been gently stirred over night, the precipitated polymer was collected and washed with methanol on a PTFE membrane filter, pore size 0.5 μm. The powder was dried under reduced pressure to afford 475 mg (30%) of the polymer, APFO-Green1 as a dark green powder. ^{1}H NMR (300 MHz, $CDCl_3$): δ 0.60–0.90 (m, 10H), 1.05–1.25 (m, 20H), 2.00–2.20 (m, 4H), 7.45–8.00 (m, 18H), 9.05–9.15 (m, 2H).

2.2. Cyclic voltammetry

Cyclic voltammetry experiments were carried out using Autolab PGStat 10 (EchoChemie, The Netherlands). A conventional three-electrode system consisting of a glassy carbon disk as working electrode, a Ag/Ag^+ quasi reference electrode and a platinum wire as counter electrode were used. The polymer films were deposited on working electrodes of glassy carbon by solvent casting. The electrode was polished by using 0.3-μm Al_2O_3 slurry followed by thorough rinsing with de-ionized water, acetone, and acetonitrile. Any remaining liquid was wiped of with a soft cloth. A 0.1 M solution of tetrabutylammonium tetrafluoroborate (Bu_4NBF_4) in acetonitrile was used as a supporting electrolyte. Nitrogen gas was bubbled through the solution for 20 min to remove dissolved oxygen and also bubbled over the solution throughout the experiment. The potential of the quasi reference electrode was corrected to the Ag/AgCl reference electrode by measuring the ferocene/ferrocenium redox couple in the supporting electrolyte-solvent system, which was found to be 0.433 V vs Ag/AgCl.

2.3. Photoluminescence measurements

A monochromatic light ($\lambda = 450$ nm) poduced by a light beam from a halogen tungsten lamp passed through a monochromator (MS 257, Oriel Instruments) was used as the monochromatic excitation light source. An integrating sphere (Labsphere IAS-040-SL) was utilized for colleting incident and emitted photons and a spectrometer equipped with a CCD device (MS 257, Oriel Instruments) was used for collecting spectra during the measurement.

2.4. Diode fabrication

Polymer solar cells were fabricated using a sandwich structure of ITO/PEDOT-PSS/APFO-Green1:PCBM (or BTPF60 or BTPF70)/LiF/Al. ITO refers to indium–tin-oxide and PEDOT-PSS to poly(ethylene dioxythiophene-polystyrenesulfonic acid), Bayer, EL grade. The polymer, APFO-Green1 blended with PCBM or BTPF (1:2–1:8 by weight) was dissolved in a chloroform/dichlorobenzene (10:1) mixture. First, PEDOT-PSS was spin-coated on top of cleaned, pre-patterned ITO coated glass substrates (sheet resistance of 20 Ω/square, Merck KGaA) as polymer anode followed by annealing at 120 °C for 5 min, leaving a 50 nm thick film. APFO-Green1 and the fullerene were deposited on top of the PEDOT-PSS by spin-coating, leaving an active layer with a thickness of 70–120 nm. Finally, the cathode consisting of LiF (1 nm) and Al (60 nm) were sequentially deposited on top of the active layer by thermal evaporation in vacuum $<10^{-6}$ Torr. The active area, defined by the overlap of the anode and cathode, was 4–6 mm^2. Thicknesses were determined using a Sloan DEKTAK 3030 surface profilmeter.

3. Results and discussion

3.1. Syntheses

The synthetic route to APFO-Green1 is outlined in Schemes 1 and 2 while the laboratory details are described in Section 2. A synthetic procedure with the same general outline as the steps outlined in Scheme 1 has been previously published [24,42]. However, all steps from the previous method have been modified to obtain an optimized procedure, which gives better yields and allows less complicated work-up.

Nitration of 4,7-dibromo-benzo[1,2,5]thiadiazole (**I**) in a 50/50 (vol/vol) of fuming nitric acid and fuming sulphuric acid gave 4,7-dibromo-5,6-dinitro-benzo[1,2,5]thiadiazole (**II**) in 29% yield after recrystallization in ethanol. This step is a modified procedure based on the nitration described by Uno et al. [42]. Although a 29% yield might seem low, the modifications both increased the yield and facilitated the work-up of the product considerably compared to the original procedure. Once pure **II** had been isolated, it was treated with 2-(tribytylstannyl)thiophene in the presence of a catalytic amount of $PdCl_2(PPh_3)_2$ to give 4,7-di-thiophen-2-yl-5,6-dinitro-benzo[1,2,5]thiadiazole (**III**) in 92% yield. **III** was then readily reduced in quantitative (100%) yield to its corresponding diamine (**V**) by heating it 4 h at 80 °C in acetic acid with a large excess of fine iron powder.

The completion of the low band-gap monomer and the polymerization of APFO-Green1 is outlined in Scheme 2. Diamine **IV** was treated with benzil in acetic acid to give the dark blue low band-gap segment **V** in 89% yield. To enable a Suzuki-type copolymerization [29], **V** was dibrominated with *N*-bromosuccinimide in a 1:1 (vol/vol) mixture of acetic acid and chloroform. This gave the low band-gap monomer **VI** in excellent yield (94%). Both these reactions are straightforward, easily monitored by thin-layer chromatography and give high yields after simple purifications (Section 2). Employing the Suzuki copolymerization procedure described by Svensson et al. [29], diboronic ester **VII** [41] and the dibrominated low band-gap segment **VI** was copolymerized. This gave APFO-Green1, an alternating copolymer of 9,9-dioctylfluorene and the low band-gap segment with a deep green color. The chloroform soluble fraction of APFO-Green1 was isolated by Soxhlet extraction in 30% yield, relative to the initial amount of monomers.

3.2. Batches and molecular weights

The polymerization procedure described in Section 2 (Batch 1) was carried out with equivalent amounts of the two monomers. However, another polymerization (Batch 2) was performed in the same manner, except for a 10% excess of the fluorene monomer, which led to a minimized formation of chloroform insoluble material. As shown in Table 1, the introduction of excess fluorene led to a considerable decrease in molecular weight due to the unbalanced stoichiometry. Despite very low molecular weights, both batches of APFO-Green1 proved very useful in devices. In the polymerization step of Batch 1, an insoluble polymer fraction, was formed. Hence, the molecular weight averages of Batch 1 reflect the chloroform soluble polymer fraction useful for device preparation.

3.3. Absorption

The optical absorption of APFO-Green1, spin-coated on a glass slide from a chloroform solution is shown in Fig. 1 where two distinct absorption bands can be observed, the first located at $300 < \lambda < 500$ nm and the second at $600 < \lambda < 1000$ nm. Based on previous studies carried out on a similar polymer [43] and recent quantum chemical modeling [44], the short wavelength absorption band is attributed to the delocalized $\pi \rightarrow \pi^*$ transition in the polymer chains while the long wavelength band should originate from a charge transfer state in the D–A–D-segment. From the onset of absorption (975 nm), the band-gap of APFO-Green1 can be estimated to 1.3 eV, the lowest number reported so far for polyfluorene copolymers. This shows that the band gap in alternating polyfluorene copolymers can be controlled by the D–A–D-segment and result in a much lower band-gap than for polyfluorene homopolymers [41]. Also, this confirms that the introduction of a stronger acceptor in the D–A–D-segment

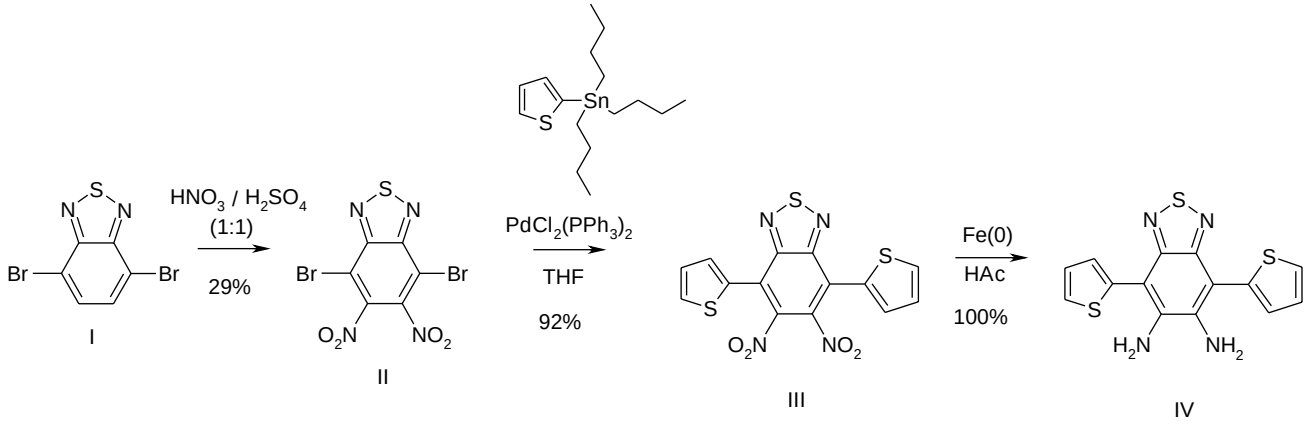

Scheme 1. Initial synthetic steps toward APFO-Green1.

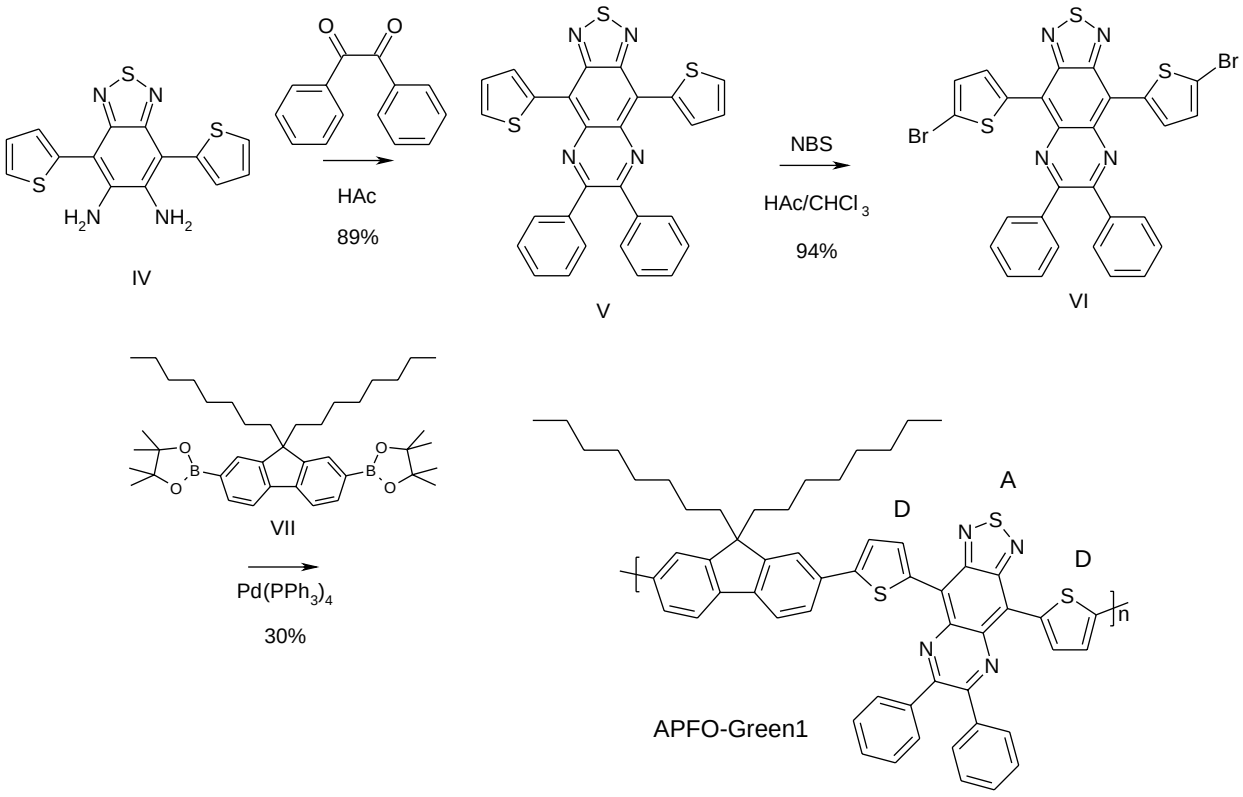

Scheme 2. APFO-Green1, final synthetic steps.

gives the polymer a lower band-gap compared to previous APFO's [29,30].

3.4. Cyclic voltammetry

Cyclic voltammetry is the simplest experimental tool to estimate the values of the highest occupied molecular orbital (HOMO), the lowest unoccupied molecular orbital (LUMO) and band gaps. The most commonly used method is based on the detailed quantum chemical studies of Bredas [45], which can be expressed as: $I_p(\text{HOMO}) = -(E_{on}^{ox} + 4.4)$ eV and $E_a(\text{LUMO}) = -(E_{on}^{red} + 4.4)$ eV where E_{on}^{ox} and E_{on}^{red} are the onset potential values in volts for oxidation and reduction processes against the Ag/AgCl reference electrode. From the cyclic voltammetry results shown in Fig. 2, the HOMO and LUMO levels of APFO-Green1 were estimated to −5.3 and −4.0 eV, respectively. This means that the band-gap from electrochemistry is determined to 1.3 eV, the same number as the one derived from onset of optical absorption.

Table 1
Batch data for APFO-Green1

Batch	Monomer ratio D–A–D: fluorene	Yield (%)	$\bar{M}_n$ [a]	$\bar{M}_w$ [a]
1	1.0:1.0	30	3600	6200
2	1.0:1.1	27	1900	3400

[a] Molecular weight averages determined by size exclusion chromatography calibrated against polystyrene standards and with 1,2,4-trichlorobenzene (135 °C) as eluent.

3.5. Photo- and electro-luminescence

Films of APFO-Green1 show photoluminescence at extended wavelengths with the spectrum (Fig. 3) peaking in the region of 1 μm. The photoluminescence quantum efficiency was determined to 1.5% in chloroform solution and approximately 0.5% in film. This photoluminescence peak is among the longest wavelengths reported from conjugated polymers to date and makes this class of polymers interesting for near-IR emitting diode applications. Diodes fabricated from APFO-Green1 show electro-luminescence spectra peaking in the same near-IR region as the photoluminescence spectrum [36]. By incorporation of this emphasized D–A–D segment, which maintains a planar structure in the polymer backbone, APFO-Green1 has a low band-gap, which results in these extended luminescence wavelengths.

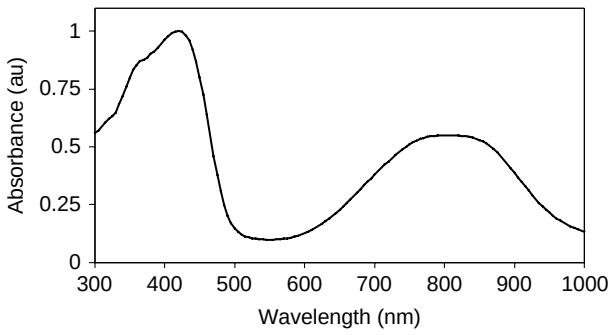

Fig. 1. Absorption spectrum of APFO-Green1, spin-coated from a chloroform solution.

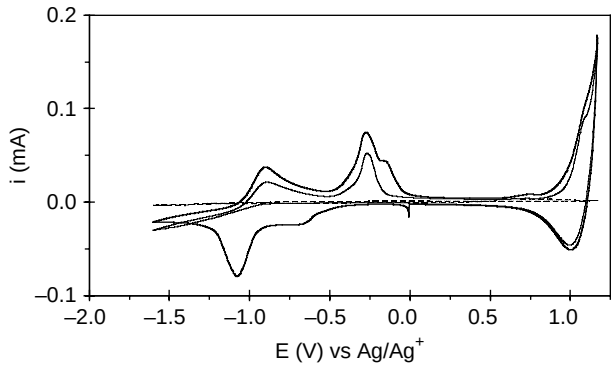

Fig. 2. Cyclic voltammogram showing first scan (thin), third scan (thick), and background scan (dashed) of APFO-Green1 cast on a glassy carbon electrode.

3.6. Solar cell performance

Several attempts to fabricate solar cells based on APFO-Green1 blended with PCBM [17] resulted in inferior devices with low photovoltaic performances. The explanation for this poor behavior is quite logical. By introducing a strong electron acceptor in the D–A–D-segment of the polymer, the energy difference, and thereby the driving force for electron transfer, between the polymer LUMO and the PCBM LUMO has become too low. This is confirmed when comparing the LUMO level of APFO-Green1, determined herein to −4.0 eV from cyclic voltammetry, to that of PCBM, which has been reported between −3.7 and −3.8 eV [46,47]. To circumvent this setback, PCBM was substituted for a fullerene with stronger electron affinity, BTPF60 [39,48] with its LUMO located at approximately −4.1 eV.

Solar cells with APFO-Green1:BTPF60 blends as active layer show a distinctive increase in performance compared to those based on APFO-Green1:PCBM [39]. The onset of photocurrent generation, shown in Fig. 4, is in the region of 1 μm and an EQE-maximum of 8.4% is located at approximately 840 nm. Since, BTPF60 exhibits practically no absorption above 500 nm [39], the photocurrent generation at long wavelengths must originate from absorption by the polymer. This is further confirmed by the similarities between the absorption curve of the polymer (Fig. 1) and the EQE-data for APFO-Green1:BTPF60 shown in Fig. 4. When irradiating a device of this type with simulated sunlight (AM1.5, 100 mW/cm^2), an overall power conversion efficiency (PCE) of 0.3% was reached.

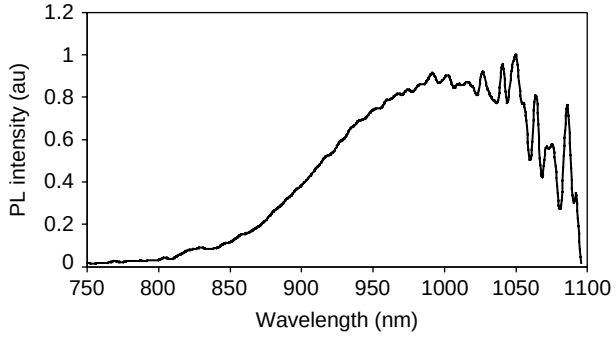

Fig. 3. Photoluminescence spectrum of APFO-Green1 excited at 450 nm.

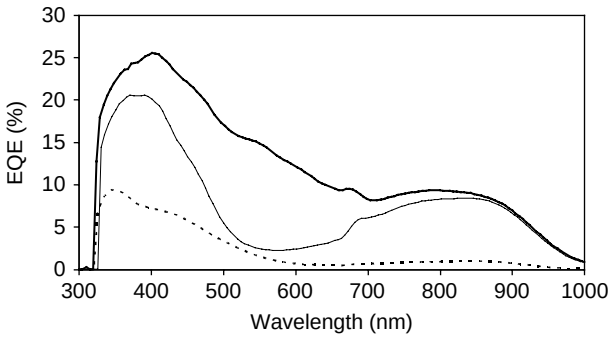

Fig. 4. Photocurrent spectral response (EQE, external quantum efficiency) of solar cells based on APFO-Green1:PCBM (dashed) APFO-Green1:BTPF60 (thin) and APFO-Green1:BTPF70 (thick).

Despite the promising results obtained for APFO-Green1:BTPF60 devices in the long wavelength region, the poor absorption in the intermediate wavelength region (∼500–700 nm) leads to rather low quantum efficiencies at these wavelengths. To compensate for this, solar cells with BTPF70 [40], the C70 equivalent of BTPF60, were fabricated.

The electrochemical properties of BTPF70 are similar (LUMO = −4.2 eV) to those of BTPF60 but, BTPF70 absorbs light in the intermediate wavelength region (∼500–700 nm), where neither BTPF60, nor APFO-Green1 shows any significant absorption. Solar cells based on APFO-Green1:BTPF70 blends exhibit enhanced photovoltaic responses (Fig. 4) at short and intermediate wavelengths, while maintaining the high EQE-values in the long wavelength region. Power conversion efficiencies of 0.7% were achieved under the illumination of simulated sunlight (AM1.5, 100 mW/cm^2) [40].

3.7. Annealing

It has been shown that heat treatment (annealing) can induce a liquid crystalline state in polyfluorenes [35] and by annealing APFO-Green1, an ordered, liquid crystalline like state is obtained. This is confirmed by studying a polymer sample, placed between crossed polarizers in a light microscope while heating. When a powder of the polymer (Batch 1) is heated to 240 °C, the powder slowly softens. Upon further heating (270 °C), the polymer starts showing optical activity. At 310 °C, the optical activity has disappeared completely but when the temperature is brought back down below 300 °C, the optical activity re-appears. This ordering is then preserved when the sample is allowed to cool to room temperature. For Batch 2, which has a lower molecular weight, the optical activity appears at 190 °C and disappears above 240 °C. For both batches, these temperatures are well below the decomposition temperatures determined by thermogravimetric analysis, see Table 2. Also, the transition from the liquid crystalline like state to isotropic melt was detected by differential scanning calorimetry for both batches and the results are shown in Table 2. The ordered state has been utilized to achieve

Table 2
Thermal data for APFO-Green1

Batch	T_{d5}[a] (°C)	$T_{LC,opt}$[b] (°C)	$T_{Iso,opt}$[c] (°C)	$T_{Iso,DSC}$[d] (°C)
1	400	270	300	296
2	298	190	240	237

[a] Decomposition temperature (5% weight loss) determined by thermogravimetric analysis under N_2 atmosphere.
[b] Temperature at which optical activity appears. Determined by light microscopy with crossed polarizers.
[c] Temperature at which optical activity disappears and the polymer melt becomes isotropic. Determined by light microscopy with crossed polarizers.
[d] The isotropic transition temperature determined by differential scanning calorimetry.

improved transistor properties by enhancing the hole mobility to 3×10^{-3} $cm^2/V\,s$ by thermal treatment of thin film transistors with APFO-Green1 (Batch 2) as active layer [38]. Recent results from transistors with Batch 1 of APFO-Green1 show one order of magnitude higher hole mobilities [37]. This shows that high hole mobilities can be reached in donor–acceptor polymers.

4. Conclusion

An alternating polyfluorene copolymer, APFO-Green1, containing a low band-gap donor–acceptor–donor (D–A–D) segment has been designed and synthesized for use in optoelectronic devices. The band-gap of the polymer was estimated to 1.3 eV. Absorption and photovoltaic response at extended wavelengths were obtained in composites with fullerenes. This opens up possibilities of using conjugated polymers to fabricate efficient NIR photodiodes and multi layer solar cells covering most of the solar spectrum. Additionally, APFO-Green1 shows photo- and electro-luminescence spectra peaking in the region of 1 μm and high hole mobility in thin film transistors. The absorption and photovoltaic response in the infrared region combined with high charge mobility makes this class of conjugated polymers promising for plastic solar cell applications.

Acknowledgements

The support from the Swedish Ministry of Education, Swedish Research Council, and Swedish Foundation of Strategic Research are gratefully acknowledged. The authors also thank Prof. F Langa for supplying the fullerenes.

Supplementary data

Supplementary data associated with this article can be found at doi:10.1016/j.polymer.2006.03.110.

References

[1] Burroughes JH, Bradley DDC, Brown AR, Marks RN, Mackay K, Friend RH, et al. Nature 1990;347(6293):539–41.
[2] Tessler N, Denton GJ, Friend RH. Nature 1996;382(6593):695–7.
[3] Dimitrakopoulos CD, Malenfant PRL. Adv Mater 2002;14(2):99–117.
[4] Sariciftci NS, Braun D, Zhang C, Srdanov VI, Heeger AJ, Stucky G, et al. Appl Phys Lett 1993;62(6):585–7.
[5] Wnek GE, Chien JCW, Karasz FE, Lillya CP. Polymer 1979;20(12):1441–3.
[6] Fukuda M, Sawada K, Yoshino K. Jpn J Appl Phys, Part 2: Lett 1989;28(8):L1433–L5.
[7] Langer JJ. Synth Met 1987;20(1):35–41.
[8] Tourillon G, Garnier F. J Electroanal Chem Interfacial Electrochem 1982;135(1):173–8.
[9] Sirringhaus H, Tessler N, Friend RH. Science 1998;280(5370):1741–4.
[10] Bao Z, Feng Y, Dodabalapur A, Raju VR, Lovinger AJ. Chem Mater 1997;9(6):1299–301.
[11] Shaw JM, Seidler PF. IBM J Res Dev 2001;45(1):3–9.
[12] MacDiarmid AG. Angew Chem, Int Ed 2001;40(14):2581–90.
[13] Dodabalapur A, Bao Z, Makhija A, Laquindanum JG, Raju VR, Feng Y, et al. Appl Phys Lett 1998;73(2):142–4.
[14] Drury CJ, Mutsaers CMJ, Hart CM, Matters M, de Leeuw DM. Appl Phys Lett 1998;73(1):108–10.
[15] Brabec CJ. Sol Energy Mater Sol Cells 2004;83(2–3):273–92.
[16] Schilinsky P, Waldauf C, Hauch J, Brabec CJ. Thin Solid Films 2004;451–452:105–8.
[17] Hummelen JC, Knight BW, LePeq F, Wudl F, Yao J, Wilkins CL. J Org Chem 1995;60(3):532–8.
[18] Andersson MR, Thomas O, Mammo W, Svensson M, Theander M, Inganäs O. J Mater Chem 1999;9(9):1933–40.
[19] van Mullekom HAM, Vekemans JAJM, Havinga EE, Meijer EW. Mater Sci Eng, Rep 2001;R32(1):1–40.
[20] Berggren M, Gustafsson G, Inganäs O, Andersson MR, Wennerstrom O, Hjertberg T. Appl Phys Lett 1994;65(12):1489–91.
[21] Wudl F, Srdanov G. US Patent 5189136; 1993.
[22] Grimsdale AC, Cacialli F, Gruener J, Li X-C, Holmes AB, Moratti SC, et al. Synth Met 1996;76(1–3):165–7.
[23] Greenham NC, Samuel IDW, Hayes GR, Phillips RT, Kessener YARR, Moratti SC, et al. Chem Phys Lett 1995;241(1,2):89–96.
[24] Kitamura C, Tanaka S, Yamashita Y. Chem Mater 1996;8(2):570–8.
[25] Cravino A, Loi MA, Scharber MC, Winder C, Neugebauer H, Denk P, et al. Synth Met 2003;137(1–3):1435–6.
[26] Zhang F, Perzon E, Wang X, Mammo W, Andersson MR, Inganaes O. Adv Funct Mater 2005;15(5):745–50.
[27] Winder C, Sariciftci NS. J Mater Chem 2004;14(7):1077–86.
[28] Campos LM, Tontcheva A, Guenes S, Sonmez G, Neugebauer H, Sariciftci NS, et al. Chem Mater 2005;17(16):4031–3.
[29] Svensson M, Zhang F, Inganäs O, Andersson MR. Synth Met 2003;135–136:137–8.
[30] Svensson M, Zhang F, Veenstra SC, Verhees WJH, Hummelen JC, Kroon JM, et al. Adv Mater 2003;15(12):988–91.
[31] Inganäs O, Svensson M, Zhang F, Gadisa A, Persson NK, Wang X, et al. Appl Phys A 2004;79(1):31–5.
[32] Halls JJM, Arias AC, MacKenzie JD, Wu W, Inbasekaran M, Woo EP, et al. Adv Mater 2000;12(7):498–502.
[33] Scherf U, List EJW. Adv Mater 2002;14(7):477–87.
[34] Bernius MT, Inbasekaran M, O'Brien J, Wu W. Adv Mater 2000;12(23):1737–50.
[35] Grell M, Bradley DDC, Inbasekaran M, Woo EP. Adv Mater 1997;9(10):798–802.
[36] Chen M, Perzon E, Andersson MR, Marcinkevicius S, Jonsson SKM, Fahlman M, et al. Appl Phys Lett 2004;84(18):3570–2.
[37] Chen M, Crispin X, Perzon E, Andersson MR, Pullerits T, Andersson M, et al. Appl Phys Lett 2005;87(25):252105/252101–252105/252103.
[38] Chen MX, Perzon E, Robisson N, Joensson SKM, Andersson MR, Fahlman M, et al. Synth Met 2004;146(3):233–6.
[39] Wang X, Perzon E, Delgado JL, De la Cruz P, Zhang F, Langa F, et al. Appl Phys Lett 2004;85(21):5081–3.
[40] Wang X, Perzon E, Oswald F, Langa F, Admassie S, Andersson MR, et al. Adv Funct Mater 2005;15(10):1665–70.

[41] Ranger M, Rondeau D, Leclerc M. Macromolecules 1997;30(25): 7686–91.
[42] Uno T, Takagi K, Tomoeda M. Chem Pharm Bull 1980;28(6): 1909–12.
[43] Jespersen KG, Beenken WJD, Zaushitsyn Y, Yartsev A, Andersson M, Pullerits T, et al. J Chem Phys 2004;121(24):12613–7.
[44] Persson N-K, Sun M, Kjellberg P, Pullerits T, Inganas O. J Chem Phys 2005;123(20):204718/204711–204718/204719.
[45] Bredas JL, Silbey R, Boudreaux DS, Chance RR. J Am Chem Soc 1983; 105(22):6555–9.
[46] Brabec CJ, Cravino A, Meissner D, Sariciftci NS, Rispens MT, Sanchez L, et al. Thin Solid Films 2002;403–404:368–72.
[47] Mihailetchi VD, Blom PWM, Hummelen JC, Rispens MT. J Appl Phys 2003;94(10):6849–54.
[48] Delgado JL, de la Cruz P, Lopez-Arza V, Langa F. Tetrahedron Lett 2004; 45(8):1651–4.